



**HAL**  
open science

## Transient performance evaluation of waste heat recovery rankine cycle based system for heavyduty trucks

Vincent Grelet, Thomas Reiche, Vincent Lemort, Madiha Nadri, Pascal Dufour

### ► To cite this version:

Vincent Grelet, Thomas Reiche, Vincent Lemort, Madiha Nadri, Pascal Dufour. Transient performance evaluation of waste heat recovery rankine cycle based system for heavyduty trucks. Applied Energy, 2016, 165 (1), pp.878-892. 10.1016/j.apenergy.2015.11.004 . hal-01265044

**HAL Id: hal-01265044**

**<https://hal.science/hal-01265044>**

Submitted on 30 Jan 2016

**HAL** is a multi-disciplinary open access archive for the deposit and dissemination of scientific research documents, whether they are published or not. The documents may come from teaching and research institutions in France or abroad, or from public or private research centers.

L'archive ouverte pluridisciplinaire **HAL**, est destinée au dépôt et à la diffusion de documents scientifiques de niveau recherche, publiés ou non, émanant des établissements d'enseignement et de recherche français ou étrangers, des laboratoires publics ou privés.



Distributed under a Creative Commons Attribution 4.0 International License

**This document must be cited according  
to its final version which is published in a journal as:**

**V. Grelet , T. Reiche, V. Lemort, M. Nadri, P. Dufour,  
"Transient performance evaluation of waste heat recovery rankine cycle based  
system for heavyduty trucks",  
Applied Energy, 2016, 165(1), pp. 878–892.  
[DOI : 10.1016/j.apenergy.2015.11.004](https://doi.org/10.1016/j.apenergy.2015.11.004)**

**You downloaded this document from the  
CNRS open archives server, on the webpages of Pascal Dufour:  
<http://hal.archives-ouvertes.fr/DUFOUR-PASCAL-C-3926-2008>**

# TRANSIENT PERFORMANCE EVALUATION OF WASTE HEAT RECOVERY RANKINE CYCLE BASED SYSTEM FOR HEAVY DUTY TRUCKS

Vincent Grelet<sup>a,b,c</sup>, Thomas Reiche<sup>a</sup>, Vincent Lemort<sup>b,\*</sup>, Madiha Nadri<sup>c</sup>,  
Pascal Dufour<sup>c</sup>

<sup>a</sup>*Volvo Trucks Global Trucks Technology Advanced Technology and Research, 1 av Henri  
Germain 69800 Saint Priest, France, (vincent.grelet@volvo.com,  
thomas.reiche@volvo.com).*

<sup>b</sup>*LABOTHAP, University of Liege, Campus du Sart Tilman Bat. B49 B4000 Liege,  
Belgium, (vincent.lemort@ulg.ac.be).*

<sup>c</sup>*Universite de Lyon, F-69622, Lyon, France, Universite Lyon 1, Villeurbanne, France,  
CNRS, UMR 5007, LAGEP, (nadri@lagep.univ-lyon1.fr, dufour@lagep.univ-lyon1.fr).*

---

## Abstract

The study presented in this paper aims to evaluate the transient performance of a waste heat recovery Rankine cycle based system for a heavy duty truck and compare it to steady state evaluation. Assuming some conditions to hold, simple thermodynamic simulations are carried out for the comparison of several fluids. Then a detailed first principle based model is also presented. Last part is focused on the Rankine cycle arrangement choice by means of model based evaluation of fuel economy for each concept where the fuels savings are computed using two methodologies. Fluid choice and concept optimization are conducted taking into account integration constraints (heat rejection, packaging ...). This paper shows the importance of the modeling phase when designing Rankine cycle based heat recovery systems and yields a better understanding when it comes to a vehicle integration of a Rankine cycle in a truck.

*Keywords:* Waste heat recovery system, Modeling, Thermodynamic,

---

\*Corresponding author

1 **1. INTRODUCTION**

2 Even in nowadays heavy duty (HD) engines, which can reach 45% of effi-  
3 ciency, a high amount of the chemical energy contained in the fuel is released  
4 as heat to the ambient. Driven by future emissions legislation and increase  
5 in fuel prices, engine gas heat recovering has recently attracted a lot of inter-  
6 est. Over the last decades, most of the research has focused on waste heat  
7 recovery systems (WHRS) based on the Rankine cycle [1, 2, 3]. These sys-  
8 tems can lead to a decrease in fuel consumption and lower engine emissions  
9 [4, 5]. Recent studies have brought a significant potential for such systems  
10 in a HD vehicle [6, 7]. However, before the Rankine cycle based system can  
11 be applied to commercial vehicles, the challenges of its integration have to  
12 be faced. The work done in [8] and [9] show that one of the main limita-  
13 tion is the cooling capacity of the vehicle. But other drawbacks, such as the  
14 back pressure, weight penalty or transient operation should not be minimized  
15 [10, 11]. Before tackling the problem of the control strategy of this system  
16 [12, 4], the architecture and components need to be selected to achieve a  
17 certain objective that could be to maximize the fuel savings or minimize the  
18 impact on the vehicle. This study focuses more on maximizing the system  
19 performance by taking into account the different penalties induced by the  
20 integration of the system on a heavy duty truck. Technical challenges and  
21 optimization of stationary organic Rankine cycles (ORC) are well addressed  
22 [13, 14] but for mobile applications only few studies deal with fuel saving po-  
23 tential of WHRS on dynamic driving cycles [15, 16] and the latter is generally  
24 reduced to a certain number of steady state engine operating points [17, 18].  
25 This last approach leads to an overestimation of the WHRS performance [3]  
26 and therefore of the fuel economy. In [19] different concepts are analyzed  
27 taking into account the system integration into the vehicle cooling module.  
28 The concepts differ in the number of heat sources used and the temperature  
29 level of the cooling fluid. Each is simulated on different steady state engine  
30 operating points and the fuel economy is calculated taking into account the  
31 increase in cooling fan consumption, exhaust back pressure or intake manifold  
32 temperature. Depending on the Rankine configuration and the location of  
33 the condenser, improvements from 2.2% (recovering heat only from exhaust

34 gases and condenser placed in front of the cooling package) to 6.9% (exhaust  
35 gas recirculation and exhaust heat are recovered and condenser is fed with  
36 engine coolant) are achieved. In [15], dynamic fuel economy is evaluated  
37 on a light duty vehicle taking into account the main penalties induced by  
38 the integration of the WHRS. Fuel savings from 3.4% to 1.3% are presented  
39 depending on the level of integration of the system into the vehicle architec-  
40 ture. However, no optimization is proposed either on the system architecture  
41 or on the condenser integration into the cooling package. This paper is or-  
42 ganized as follows. The second section explains the different considerations  
43 to take when designing a Rankine cycle for a HD application. In the third  
44 section, the different models used in the rest of the study are explained. In  
45 the fourth section, the scope of the study and the different methodologies are  
46 explained. In the fifth section, simulation results are analyzed and possible  
47 improvements are proposed. Finally, conclusions are drawn and directions  
48 for future research work are discussed.

## 49 **2. DESIGN ASPECTS TO CONSIDER**

50 Figure 1 shows a simple waste heat recovery system mounted on a 6 cylinder  
51 heavy duty engine. Working fluid flows through four basic components which  
52 are: the pump, the evaporator linked to the heat source, the expansion ma-  
53 chine and the condenser linked to the heat sink. For sake of clarity, the link  
54 between the expander and the engine driveline is represented by a dashed  
55 line since it can be either mechanical or electrical (by coupling a generator to  
56 the expansion machine and reinject the electricity on the on board network).  
57

### 58 *2.1. Working fluid choice*

59 There are several aspects to take into account when choosing a working  
60 fluid for this application. Unlike stationary power plants where the main  
61 consideration is the output power or the efficiency, here other aspects have to  
62 be considered such as fluid deterioration, environmental aspects or freezing.  
63 Up to now, several studies have tried to identify the ideal fluid for WHRS  
64 [20, 21, 22] but no single fluid has been found. Recently, new performance  
65 indicators have been introduced [14, 23], where cost and design issues enter  
66 into consideration.

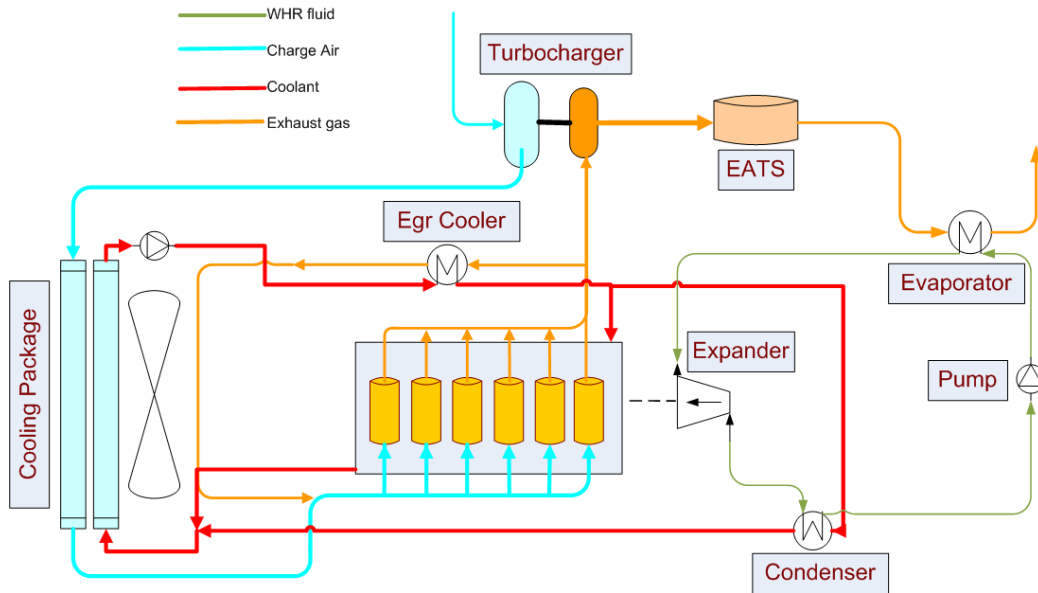


Figure 1: Simple waste heat recovery Rankine based system

67 *2.2. Heat sources*

68 On a commercial vehicle, a certain number of heat sources can be found  
 69 such as exhaust gases, cooling water or engine oil. These ones have several  
 70 grade of quality (temperature level) and quantity (amount of energy). If the  
 71 number of heat sources often yields higher fuel savings, it also brings more  
 72 complexity and more challenges for the design of the system (fluid, expansion  
 73 machine, control).

74 *2.3. Heat sink*

75 On a HD Truck, the only heat sink available is the vehicle cooling package  
 76 which is a module including radiators for the compressed air and the engine  
 77 coolant and cooled down by means of the ram air effect and the cooling  
 78 fan. Integration of a WHRS into the cooling module results on a higher load  
 79 on the latter and limits the amount of waste heat that can be converted  
 80 into useful work. As such, complete system analysis is necessary to find the  
 81 optimal way of recovering heat from a vehicle.

82 *2.4. Subsystem interaction*

83 The engine operation is influenced by the introduction of a WHRS. For ex-  
84 ample, as the WHRS shares the cooling system of the vehicle, the charge air  
85 cooling capacity can be lower, which has a negative behavior on the engine  
86 performance. Another example is the use of exhaust gas recirculation (EGR)  
87 as heat source. This leads to a trade-off between EGR cooling and Rank-  
88 ine cycle performance, which could impact negatively the engine emissions.  
89 Several other interactions such as the exhaust back pressure or the weight  
90 penalty could be cited.

91 The WHRS performance, and so the fuel economy induced by this later, is  
92 then dependent on all these aspects. It is therefore critical to model the  
93 complete system and its environment in order to optimize its architecture. It  
94 helps to select the best design and reduce the number of experimental tests  
95 to carry out.

96 **3. RANKINE MODELING**

97 *3.1. Rankine process*

98 The Temperature Entropy (T-s) diagram represented in figure 2 shows the  
99 associated state changes of the working fluid through the Rankine cycle:

- 100 • The pressure of the liquid is increased by the pump work up to the  
101 evaporating pressure ( $1 \rightarrow 2$ ).
- 102 • The pressurized working fluid is pre-heated ( $2 \rightarrow 3a$ ), vaporized ( $3a \rightarrow$   
103  $3b$ ) and superheated ( $3b \rightarrow 3c$ ) in a heat exchanger, by recovering heat  
104 ( $\dot{Q}_{in}$ ) from the heat source.
- 105 • The superheated vapor expands from evaporating pressure to condens-  
106 ing pressure ( $3c \rightarrow 4$ ) in an expansion device creating mechanical power  
107 ( $\dot{W}_{out}$ ).
- 108 • The expanded vapor condenses ( $4 \rightarrow 1$ ) through a condenser (linked to  
109 the heat sink) releasing heat ( $\dot{Q}_{out}$ ).

110 In this process the changes of states in both the pump and the expander are  
111 irreversible and increase the fluid entropy to a certain extent. To correctly  
112 assess the performance of a system based on the Rankine cycle, two different

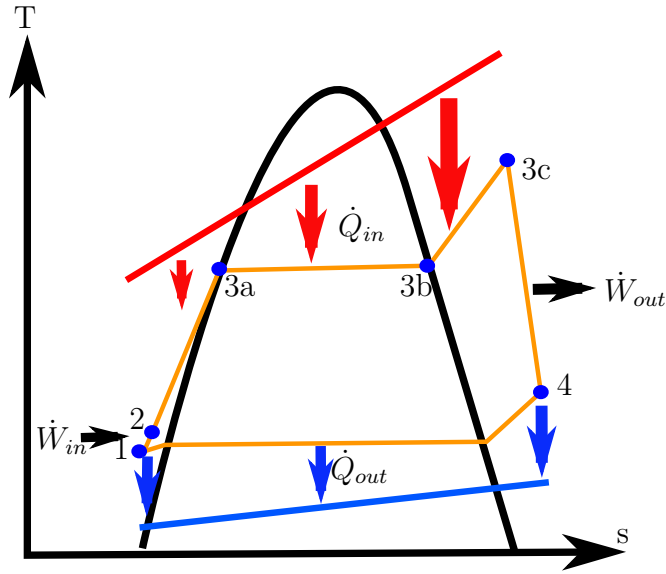


Figure 2: Temperature-Entropy diagram of the Rankine cycle

113 models have been developed: a simple 0D steady state model based on the  
 114 enthalpy change that undergoes the working fluid which does not intend to  
 115 represent components performance and where the dynamic is not taken into  
 116 account and a second, based on conservation principles applied on one spatial  
 117 dimension. This is required to represent real performance of the components  
 118 constituting the system either in steady state or in transient.

### 119 3.2. 0D steady state modeling of a Rankine cycle

120 In order to simulate a high number of working fluids, a 0D model of a Rankine  
 121 cycle using one heat source is developed. It does not represent a real system  
 122 but it allows a fast assessment of a various number of working fluids. It helps  
 123 to select the suitable working fluids for the studied application. This model  
 124 is based on the enthalpy changes in the process described in section 3.1.  
 125 This model is able to perform either subcritical or supercritical cycle, which  
 126 avoids the vaporization process and leads to a smaller system and a better  
 127 heat recovery process [24]. Those relations are verified as long as the heat  
 128 losses in the system and in the components are neglected. The 0D model

129 used is given by the system of equations (1):

$$\left\{ \begin{array}{l}
 P_{cond} = P_{sat}(T_{cond}), \\
 P_{f_{in},pump} = P_{cond}, \\
 T_{f_{in},pump} = T_{sat}(P_{f_{in},pump}) - \Delta T_{subcooling}, \\
 h_{f_{in},pump} = h(T_{f_{in},pump}, P_{f_{in},pump}), \\
 s_{f_{in},pump} = s(h_{f_{in},pump}, P_{f_{in},pump}), \\
 P_{f_{out},pump} = P_{evap}, \\
 h_{f_{out},pump} = h_{f_{in},pump} + \frac{(h_{f_{out},pump_{is}} - h_{f_{in},pump})}{\eta_{pump_{is}}}, \\
 T_{f_{out},pump} = T(h_{f_{out},pump}, P_{f_{out},pump}), \\
 s_{f_{out},pump} = s(h_{f_{out},pump}, P_{f_{out},pump}), \\
 P_{f_{out},boiler} = P_{f_{out},pump}, \\
 h_{f_{out},boiler} = h_{f_{out},pump} + \frac{\dot{Q}_{gas}}{\dot{m}_f}, \\
 T_{f_{out},boiler} = T(h_{f_{out},boiler}, P_{f_{out},boiler}), \\
 s_{f_{out},boiler} = s(h_{f_{out},boiler}, P_{f_{out},boiler}), \\
 P_{f_{out},exp} = P_{cond}, \\
 h_{f_{out},exp} = h_{f_{out},boiler} + (h_{f_{out},boiler} - h_{f_{out},exp_{is}})\eta_{exp_{is}}, \\
 s_{f_{out},exp} = s(h_{f_{out},exp}, P_{f_{out},exp}), \\
 P_{f_{out},cond} = P_{f_{out},exp}, \\
 T_{f_{out},cond} = T_{sat}(P_{f_{out},cond}) - \Delta T_{subcooling}, \\
 h_{f_{out},cond} = h(T_{f_{out},cond}, P_{f_{out},cond}), \\
 s_{f_{out},cond} = s(h_{f_{out},cond}, P_{f_{out},cond}).
 \end{array} \right. \quad (1)$$

130 where

$$\left\{ \begin{array}{l}
 h_{f_{out},pump_{is}} = h'(P_{f_{out},pump}, s_{f_{in},pump}), \\
 \dot{Q}_{gas} = \dot{m}_{gas} c_{p_{gas}} * (T_{gas_{in},boiler} - T_{gas_{out},boiler}), \\
 h_{f_{out},exp_{is}} = h'(P_{f_{out},exp}, s_{f_{out},boiler}), \\
 h_{f_{out},exp} \geq h''(x_{f_{out},exp_{min}}, P_{f_{out},exp}).
 \end{array} \right. \quad (2)$$

131 In table 1 one can find the simulation model parameters, and the abbrevia-  
 132 tions are given in the appendix. In addition to that, a routine verifying that  
 133 the pinch point ( $PP$ ) is respected during the evaporation process. Refprop  
 134 database [25] is used to compute the following quantity:  $h$ ,  $s$ ,  $T$ ,  $P_{sat}$  and  
 135  $T_{sat}$ . Input variables of the model (1) are the gas mass flow and temperature  
 136 (denoted by  $\dot{m}_{gas}$  and  $T_{gas_{in},boiler}$ ) entering in the system and the condensing  
 137 temperature ( $T_{cond}$ ). Outputs of the model are the power produced by the

Model parameters	Variable in (1)	unit	value
Pump isentropic efficiency	$\eta_{pumpis}$	%	65
Expander isentropic efficiency	$\eta_{expis}$	%	70
Maximum evaporating pressure	$P_{evap}$	bar	40
Minimum condensing pressure	$P_{cond}$	bar	1
Maximum pressure ratio	$\frac{P_{evap}}{P_{cond}}$	-	40:1
Pinch points HEX	$PP$	K	10
Pressure ratio among HEX	$\frac{P_{f_{out,boiler}}}{P_{f_{out,pump}}}$	-	1
Minimum quality after expansion	$x_{f_{out,exp,min}}$	-	0.9

Table 1: 0D model parameters

138 expansion  $\dot{W}_{exp}$ , the power consumed by the compression  $\dot{W}_{pump}$  and the  
139 net output power  $NOP$  which are defined as:

$$\begin{cases} NOP &= \dot{W}_{exp} - \dot{W}_{pump}, \\ \dot{W}_{exp} &= \dot{m}_f * (h_{f_{in,exp}} - h_{f_{out,exp}}), \\ \dot{W}_{pump} &= \dot{m}_f * (h_{f_{in,pump}} - h_{f_{out,pump}}). \end{cases} \quad (3)$$

140 The model 1 is not dynamic and does not represent any real components  
141 performance. A dynamic 1D model is therefore developed to evaluate the  
142 system performance on more realistic dynamic driving conditions.

### 143 3.3. 1D dynamic modeling of a Rankine cycle

#### 144 3.3.1. Tank

145 The reservoir is modeled by a fixed volume, which can be either vented to  
146 the atmosphere or be hermetic (depending on the condensing pressure) in  
147 order to avoid sub atmospheric conditions. Mass and energy conservation  
148 equations are:

$$\begin{cases} \dot{m}_{f_{out,tank}} - \dot{m}_{f_{in,tank}} &= \frac{\partial m_{f_{tank}}}{\partial t}, \\ \dot{m}_{f_{in,tank}} h_{f_{in,tank}} - \dot{m}_{f_{out,tank}} h_{f_{out,tank}} &= m_{f_{tank}} \frac{\partial h_{f_{tank}}}{\partial t}. \end{cases} \quad (4)$$

149 *3.3.2. Working fluid pump*

150 The working fluid pump is simply represented by a fixed displacement and  
151 isentropic efficiency. The volumetric efficiency is a function of the outlet  
152 pressure. This law is identified thanks to experimental data:

$$\dot{m}_{f_{out,pump}} = \rho_{f_{in,pump}} \frac{N_{pump}}{60} C_{cpump} \eta_{pumpvol}. \quad (5)$$

153 The outlet enthalpy is calculated as shown in the equation for  $h_{f_{out,pump}}$  in  
154 the 0D model (1).

155 *3.3.3. Heat exchangers: Evaporator(s) and condenser(s)*

156 The models are developed to dynamically predict temperature and enthalpy  
157 of transfer and working fluid at the outlet of each heat exchanger (HEX).  
158 When coming to dynamic models of those components, two methodologies  
159 can be found in the literature: moving boundary (MB) and finite volume  
160 (FV) models. Usually more complex in terms of computational capacity  
161 needed due to the high number of system states, the FV approach has the  
162 advantage to be more powerful and robust concerning the prediction. Both  
163 approaches have been widely used in large power recovery system and control  
164 system design [26, 27, 28, 29] and results in a simplification of the heat  
165 recovery boiler/condenser geometry in a great extent (i.e. by representing  
166 the boiler by a straight pipe in pipe counterflow heat exchanger). In this  
167 study, the FV approach is preferred since it easily handles starting and shut  
168 down phases [30] when only few papers adressed those cases with a MB  
169 approach [31].

170 ***Model assumptions***

171 Several assumptions are done to simplify the problem in a great extent. These  
172 ones are usually admitted when coming to heat exchanger modeling [32, 26]:

- 173 • The transfer fluid is always considered in single phase, i.e. no conden-  
174 sation in the EGR/exhaust gases is taken into account.
- 175 • The conductive heat fluxes are neglected since the predominant phe-  
176 nomenon is the convection.
- 177 • All HEX are represented by a straight pipe in pipe counterflow heat  
178 exchanger of length  $L$ .

- 179 • Fluid properties are considered homogeneous in a volume.
- 180 • Pressure dynamics is neglected since it is very fast compared to those
- 181 of heat exchanger.

### 182 ***Governing equations***

183 Boiler(s) and condenser(s) models are based on mass and energy conservation  
184 principles.

- 185 • Working fluid (internal pipe):

$$\begin{cases} A_{cross_f} \frac{\partial \rho_f}{\partial t} + \frac{\partial \dot{m}_f}{\partial z} = 0, \\ A_{cross_f} \frac{\partial \rho_f h_f}{\partial t} + \frac{\partial \dot{m}_f h_f}{\partial z} + \dot{q}_{conv_{f_{int}}} = 0, \\ \dot{q}_{conv_{f_{int}}} = \alpha_f P e_{exch_f} (T_f - T_{wall_{int}}). \end{cases} \quad (6)$$

- 186 • Internal pipe wall: An energy balance is expressed at the wall between  
187 the working fluid and the gas and is expressed as follows:

$$\dot{Q}_{conv_{f_{int}}} + \dot{Q}_{conv_{g_{int}}} = \rho_{wall} c_{p_{wall}} V_{wall_{int}} \frac{\partial T_{wall_{int}}}{\partial t}. \quad (7)$$

- 188 • Gas side (external pipe): The energy conservation is then formulated  
189 under the following form:

$$\rho_g A_{cross_g} c_{p_g} \frac{\partial T_g}{\partial t} + c_{p_g} \dot{m}_g \frac{\partial T_g}{\partial z} + \dot{q}_{conv_{g_{int}}} + \dot{q}_{conv_{g_{ext}}} = 0, \quad (8)$$

190 where the convection on the external side is used to represent the heat  
191 losses to the ambient.

- 192 • External pipe wall: As for the internal pipe an energy balance is ex-  
193 pressed between the gas and the ambient:

$$\dot{Q}_{conv_{g_{ext}}} + \dot{Q}_{conv_{amb_{ext}}} = \rho_{wall} c_{p_{wall}} V_{wall_{ext}} \frac{\partial T_{wall_{ext}}}{\partial t}. \quad (9)$$

194 In equation (7) and (9) the convection heat flow rate ( $\dot{Q}_{conv}$ ) is expressed as:

$$\begin{aligned} \dot{Q}_{conv_{j_k}} &= \alpha_j A_{exch_{j_k}} (T_{wall_k} - T_j), \\ \text{where } j &= g, f, amb \\ \text{and } k &= int, ext. \end{aligned} \quad (10)$$

195 Furthermore, to complete the system, one need boundary and initial condi-  
 196 tions. Time-dependent boundary conditions are used at  $z = 0$  and  $z = L$   
 197 ( $t > 0$ ):

$$\dot{m}_f(t, 0) = \dot{m}_{f_0}(t), \quad (11)$$

$$h_f(t, 0) = h_{f_0}(t), \quad (12)$$

$$\dot{m}_g(t, L) = \dot{m}_{g_L}(t), \quad (13)$$

$$T_g(t, L) = T_{g_L}(t). \quad (14)$$

198 The initial conditions for the gas and wall temperatures and working fluid  
 199 enthalpy are given by ( $z \in [0, L]$ ):

$$h_f(0, z) = h_{f_{init}}(z), \quad (15)$$

$$T_{wall_{int}}(0, z) = T_{wall_{int_{init}}}(z), \quad (16)$$

$$T_g(0, z) = T_{g_{init}}(z), \quad (17)$$

$$T_{wall_{ext}}(0, z) = T_{wall_{ext_{init}}}(z), \quad (18)$$

### 200 ***Heat transfer and pressure drop***

201 To model the convection from the transfer fluid to the pipe walls and from  
 202 the internal pipe to the working fluid, a heat transfer coefficient ( $\alpha$ ) is needed.  
 203 The convection from a boundary to a moving fluid is usually represented by  
 204 the dimensionless number Nusselt ( $Nu$ ) which is the ratio of convective to  
 205 conductive heat transfer.

$$Nu(\alpha) = \frac{\alpha l}{\lambda}, \quad (19)$$

206 where  $l$  represents a characteristic length and is, in this case, the hydraulic  
 207 diameter. Numerous correlations to approach this number can be found in  
 208 the literature and are usually derived from experiments, see for example [33].  
 209 In single phase, the Gnielinski correlation is chosen for both fluids. In two  
 210 phase, Chen (for evaporation) and Shah (for condensation) correlations are  
 211 used. Pressure drop in both fluids are taken into account in order to simulate  
 212 the real performance of the system. The pressure drop can be split into three  
 213 main contributors:

$$\Delta P = \Delta P_{static} + \Delta P_{momentum} + \Delta P_{friction}, \quad (20)$$

214 where the static pressure drop ( $\Delta P_{static}$ ) is function of the change in static  
 215 head (i.e. the height), the momentum pressure drop ( $\Delta P_{momentum}$ ) depends

216 on the change on density during phase change and the friction contribution  
 217 ( $\Delta P_{friction}$ ) is function of the speed of the fluid and the considered geometry.  
 218 Table 2 shows the different correlations used depending on flow conditions.  
 219 In laminar single phase, the assumption of a constant heat flux at the wall  
 is made.

		Laminar	Turbulent
Heat transfer	Single phase	Nu = 4.36	Gnielinski
	Two phase evaporation	Chen	Chen
	Two phase condensation	Shah	Shah
Pressure drop	Single phase	Poiseuille	Blasius
	Two phase	Friedel	Friedel

Table 2: Correlations used in HEX

220

### 221 3.3.4. Valve(s)

222 The fluid flow  $\dot{m}$  through the valve is modeled using a compressible valve  
 223 equation of the form:

$$\dot{m}_{f_{in,v}} = C_{d_v} S_{eff_v} \sqrt{\rho_{f_{in,v}} P_{f_{in,v}}} \phi, \quad (21)$$

224 where the compressibility coefficient  $\phi$  is defined as:

$$\phi = \frac{2\gamma_f}{\gamma_f - 1} \left( \varphi^{\frac{2}{\gamma_f}} - \varphi^{\frac{\gamma_f+1}{\gamma_f}} \right), \quad (22)$$

with

$$\varphi = \begin{cases} \frac{P_{f_{out,v}}}{P_{f_{in,v}}} & \text{if } \frac{P_{f_{out,v}}}{P_{f_{in,v}}} > \frac{2}{\gamma_f+1} \frac{\gamma_f}{\gamma_f-1} \\ \frac{2}{\gamma_f+1} \frac{\gamma_f}{\gamma_f-1} & \text{if } \frac{P_{f_{out,v}}}{P_{f_{in,v}}} \leq \frac{2}{\gamma_f+1} \frac{\gamma_f}{\gamma_f-1}, \end{cases} \quad (23)$$

225 where  $\gamma_f$  is the ratio of the specific heats of the working fluid and depends on  
 226 the temperature and the pressure. Equation (23) means that the parameter  
 227  $\varphi$  is either the pressure ratio if the flow is subsonic or the critical pressure  
 228 ratio when the flow is supersonic.

229 *3.3.5. Expansion machine*

230 Several studies have been carried out in order to choose the correct expansion  
 231 machine for Rankine based recovery system [34, 35]. In most of them where  
 232 vehicle installation is considered, turbine expanders are preferred for their  
 233 compactness and their good performance [8, 36] since the major advantage  
 234 of volumetric expander such as piston machines is the expansion ratio [37].  
 235 Though, recent study [38] has shown turbine with expansion ratio over 40:1  
 236 on a single stage with really good performance at tolerable speed for a vehicle  
 237 installation. In this study, only a kinetic expander is modeled. The turbine  
 238 nozzle is represented by the following equation:

$$\dot{m}_{f_{in,exp}} = K_{eq} \sqrt{\rho_{f_{in,exp}} P_{f_{in,exp}} \left(1 - \frac{P_{f_{in,exp}}}{P_{f_{out,exp}}}\right)^{-2}}. \quad (24)$$

239 And the isentropic efficiency is calculated according to the following relation:

$$\eta_{exp_{is}} = \eta_{exp_{is_{max}}} \left( \frac{2c_{us}}{c_{us_{max}}} - \frac{c_{us}^2}{c_{us_{max}}^2} \right), \quad (25)$$

where

$$c_{us} = \frac{u}{c_s} = \frac{\omega_{exp} R_{exp}}{2\sqrt{h_{f_{in,exp}} - h_{f_{in,exp_{is}}}}}. \quad (26)$$

240 Model parameters are fitted using data from supplier and similarity relation  
 241 [39].

242 *3.3.6. Other heat exchanger(s)*

243 In order to describe the vehicle cooling system, the number of transfer unit  
 244 (NTU) approach is used. It is commonly adopted when it comes to single  
 245 phase heat exchanger modeling. For an air cooled radiator the following  
 246 relations are used:

$$\dot{Q}_{air} = \dot{m}_{air} c_{p_{air}} \varepsilon (T_{coolant_{in}} - T_{air_{in}}). \quad (27)$$

247 For a given geometry,  $\varepsilon$  can be calculated using correlations based on the heat  
 248 capacity ratio. By considering parallel flow configuration for the radiators,

249 the effectiveness can be written:

$$\varepsilon = \frac{1 - e^{-NTU \left(1 + \frac{(\dot{m}c_p)_{min}}{(\dot{m}c_p)_{max}}\right)}}{1 + \frac{(\dot{m}c_p)_{min}}{(\dot{m}c_p)_{max}}}, \quad (28)$$

$$\text{with } NTU = \frac{UA}{(\dot{m}c_p)_{min}}. \quad (29)$$

### 250 3.3.7. Coolant pump and fan

251 The coolant pump model used is a map-based model function of engine speed  
 252 and pressure rise. This one is sized to deliver enough subcooling even at high  
 253 engine load. The engine fan is also a map-based model delivering a given  
 254 mass flow at a given speed. The fan consumption is calculated according to:  
 255

$$\dot{W}_{fan} = C_{fan} \rho_{air} N_{eng} G_{ratio} N_{fan}^2, \quad (30)$$

256 where the coefficients  $C_{fan}$  and  $G_{ratio}$  are dependent on the fan model and  
 257 vehicle. The mass flow rate blown by the fan is mapped according to data  
 258 from supplier and depends on the fan speed and atmospheric conditions. The  
 259 air mass flow rate going through the cooling package ( $\dot{m}_{air}$ ) is a combination  
 260 of the natural air mass flow rate (corresponding to a fraction of the vehicle  
 261 speed) and the forced mass flow rate (corresponding to the mass flow blown  
 262 by the fan).

$$\dot{m}_{air} = \rho_{air} A_{cool\ pack} S r_{air} V_{vehicle} + \dot{m}_{fan}(N_{fan}, \rho_{air}), \quad (31)$$

263 where  $S r_{air}$  is the ratio between the vehicle speed and the air speed in front of  
 264 the cooling package and is either calculated via computational fluid dynamics  
 265 (CFD) or measured in a wind tunnel.

## 266 4. SYSTEM OPTIMIZATION

### 267 4.1. Key aspects

268 In this section, the degrees of freedom used to optimize the WHRS are de-  
 269 tailed:

- 270 1. Fluid choice: the fluid selection is a critical part of the system opti-  
271 mization. The correct fluid choice has to match both heat source and  
272 cold sink in order to generate as much power as possible [40, 41]. From  
273 environmental and legal points of view, the working fluid has to respect:
- 274 • Its chemical class: chlorofluorocarbons (CFCs) have been ban-  
275 ished by the Montreal Protocol and hydrochlorofluorocarbons (HCFCs)  
276 production is planned to be phased out by 2030.
  - 277 • Its presence on the global automotive declarable substance list  
278 (GADSL).
  - 279 • Its chemical properties such as the global warming potential (GWP),  
280 the ozone depletion potential (ODP) or the risk phrases (R-phrases).
  - 281 • Its classification according the national fire protection agency (NFPA)  
282 704 classification (ranking above 1 in Health or Instability class)

283 In top of that, the freezing point which has to be below 0 °C.

- 284 2. Components choice and design: the correct choice of components and  
285 particularly the expansion machine have an important impact on the  
286 system performance and the control design. Indeed, a volumetric ex-  
287 pander is less stringent in terms of degree of superheat and tolerate  
288 a given amount of liquid during the expansion process whereas a kinetic  
289 expander requires a higher degree of superheat in order to have a full  
290 vapor expansion (liquid droplets can cause blade erosion and broke the  
291 machine). The design of all other components of the Rankine system  
292 is also critical to maximize its potential. For example, too big heat  
293 exchangers show higher performance but also inertia which could be a  
294 disadvantage when coming to highly dynamic driving cycle since the  
295 more interesting points (i.e. high load engine operating points) are not  
296 lasting for long. A heavy evaporator is therefore not catching up the  
297 maximum potential of this high heat flow rate.
- 298 3. Heat sources and sinks arrangement: the architecture of sources and  
299 sinks has to be adapted to increase overall performance. Heat sources  
300 choice and arrangement impact a lot the system performance by chang-  
301 ing the heat input to the system. The cold sinks choice is influencing  
302 the condensing pressure so the overall pressure ratio (and therefore the  
303 power generated by the expander).

304 4. Other system interactions: as the final goal is to implement the system  
 305 in a heavy duty vehicle, the WHRS must be considered not as a stan-  
 306 dalone system but as a connected sub system of the complete vehicle.  
 307 The interactions of the Rankine system on the other sub-systems have  
 308 to be taken into account (e.g. increase in fan consumption due to the  
 309 heat rejection coming from the condenser).

310 *4.1.1. Investigated architectures and components*

311 Several studies have been conducted in the field of waste heat recovery Rank-  
 312 ine based systems for mobile applications. A screening of the different heat  
 313 sources available is reported in [5] and shows that the most promising ones  
 314 are the EGR and the Exhaust streams. In the present study, only these  
 315 two heat sources are considered since they present the higher grade of tem-  
 316 peratures among other sources. Therefore four different Rankine layout are  
 317 studied:

- 318 1. Exhaust recovery only where the only heat source are the exhaust gases.

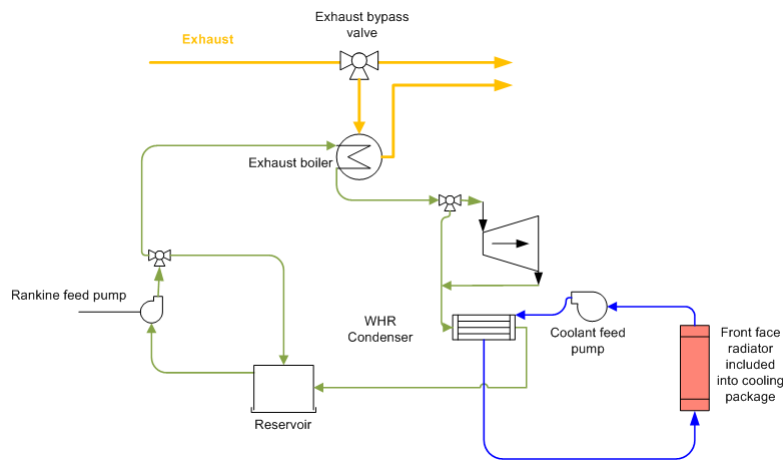


Figure 3: Exhaust only system schematic

- 319 2. EGR recovery only where only the EGR gases are used as the only heat  
 320 source.

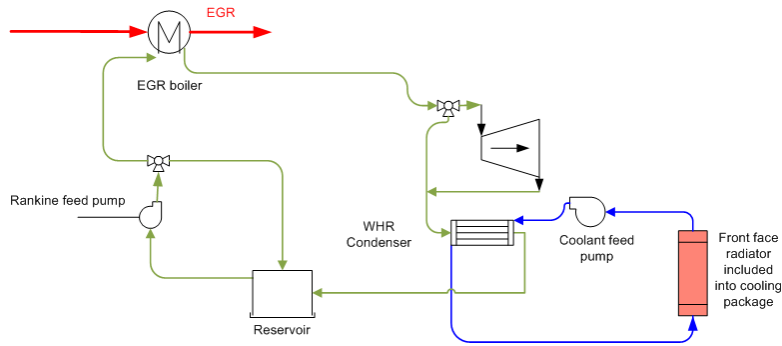


Figure 4: EGR only system schematic

- 321 3. Both sources in parallel where the working fluid is split into two streams  
 322 heated up separately by each source and then mixed before the ex-  
 323 pander.

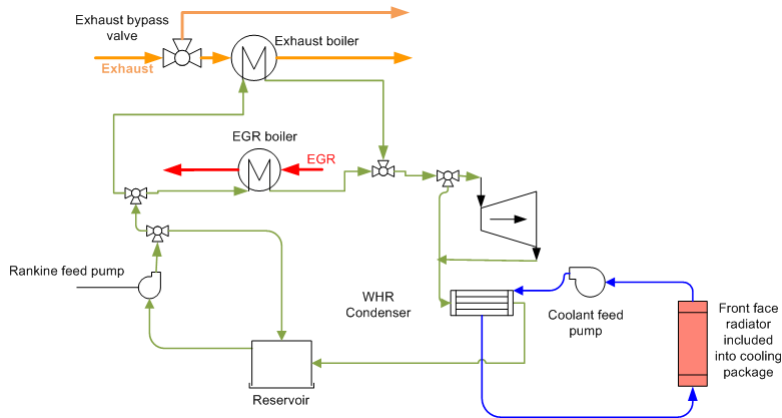


Figure 5: Exhaust and EGR in parallel system schematic

- 324 4. EGR and exhaust in series where the EGR gases are used to preheat  
 325 the fluid and the exhaust gases to vaporize and superheat. Using the  
 326 EGR as a preheater, instead of a superheater, is chosen to lower the  
 327 EGR gases temperature after the evaporation process.

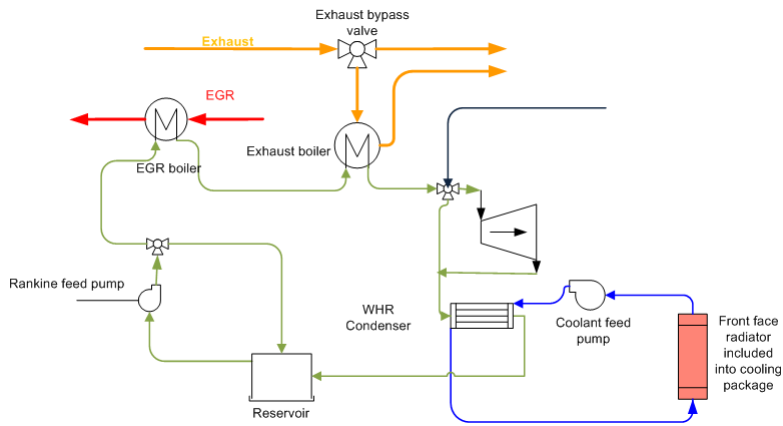


Figure 6: Exhaust and EGR in series system schematic

328 Coupled to that, two different cooling architecture are approached:

- 329 • A first one (called in the following Cooling Config 1) which uses a low  
 330 temperature radiator dedicated to the Rankine condenser and is placed  
 331 between the charge air cooler (CAC) and the engine radiator.

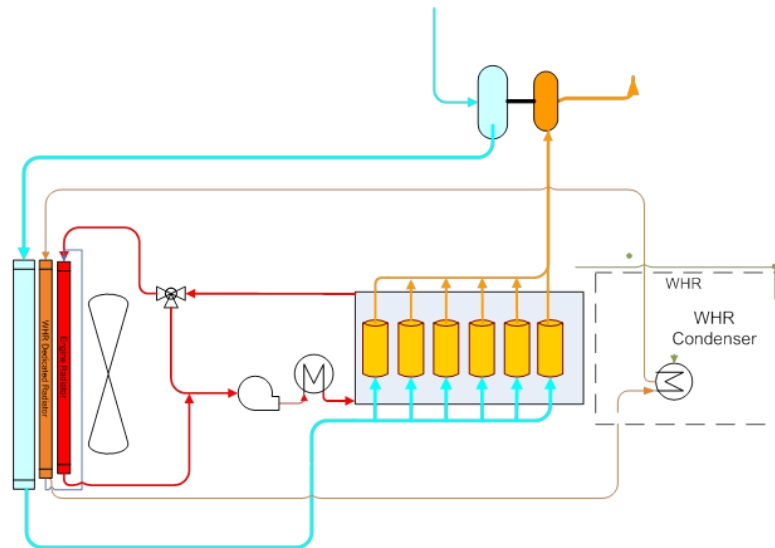


Figure 7: Cooling config 1

- 332 • A second one (called in the following Cooling Config 2) using the engine

333 coolant as heat sink for the Rankine cycle. In that case, a derivation  
 334 of the coolant is done in front of the engine to benefit from the lowest  
 335 temperature grade.

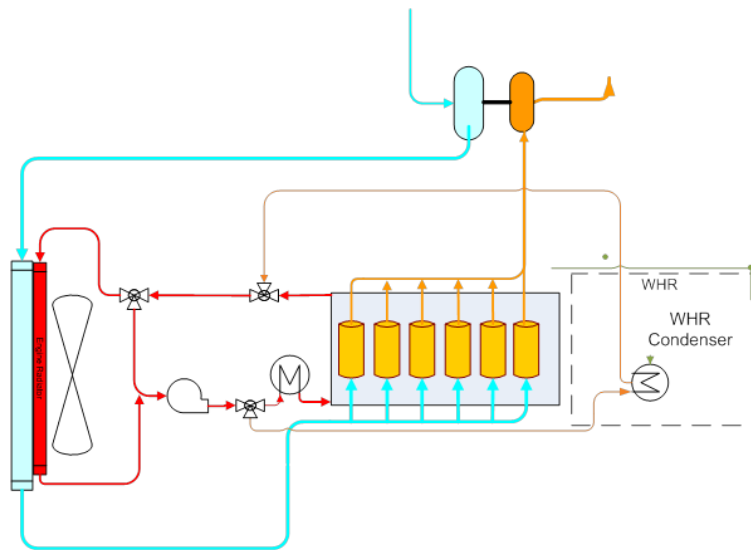


Figure 8: Cooling config 2

336 Concerning the components, as previously said, the study is limited to one  
 337 expansion machine technology: turbine expander. For the heat exchangers  
 338 (evaporator(s) and condenser), only counter-current configurations which are  
 339 usually used in this kind of applications [42] are considered.

#### 340 4.2. Duty cycles

341 Driving conditions are acting as input disturbances and therefore, their im-  
 342 pact on the target performance must be studied with care.

##### 343 4.2.1. Steady state evaluation

344 Under steady state driving conditions, the performance is evaluated by ex-  
 345 pressing the weighted average net output power of the 1D model (3.3) (the  
 346 NOP, which is the additional power that the engine receives, therefore cor-  
 347 responds to the fuel economy) on 13 engine operating points (summarized

Name	Vehicle speed	EGR mass flow	EGR temperature	Exhaust mass flow	Exhaust temperature	Weight factor
Parameter	$V_{vehicle}$	$\dot{m}_{egr}$	$T_{egr0}$	$\dot{m}_{exh}$	$T_{exh0}$	$w_i$
Unit	$km/h$	$g/s$	$^{\circ}C$	$g/s$	$^{\circ}C$	$\%$
1	20	31.5	263.1	78.7	237.9	6.9
2	85	38	409.5	119.8	338.2	9.0
3	60	59.5	635.0	309.3	443.9	4.9
4	85	54.6	544.0	252.4	413.0	2.6
5	75	46.1	454.0	154.6	366.4	18.9
6	85	56.3	247.5	85.7	212.5	10.5
7	30	85.9	631.0	352.7	425.1	2.8
8	85	69.4	562.5	290.5	405.5	3.6
9	50	58	473.0	183.2	336.2	12.7
10	85	59.8	251.0	95.2	216.0	11.2
11	45	87.1	581.0	326.8	400.8	2.3
12	75	68.9	472.0	198.4	359.6	10.7
13	85	62.9	252.5	102.8	217.5	3.9

Table 3: Steady state evaluation: Driving conditions and weight for 13 engine operating points

348 in table 3) These operating points are chosen to represent a classical long  
349 haul driving cycle and weighted according to the percentage of energy used  
350 on each operating point. Operating point number 5 is identified as the de-  
351 signing point whereas the operating points 3 and 11 are considered critical  
352 due to the high engine load and the low vehicle speed.

#### 353 4.2.2. Dynamic evaluation

354 In order to accurately assess the potential of the WHRS, dynamic driving cy-  
355 cles are also used to complete the study and check whether the performance  
356 found with the previous method is correct. This is really important when  
357 coming to thermal systems performance estimation since they generally have  
358 long response time [43]. The driving cycle used is split into 7 phases (sum-  
359 marized in table 4) supposed to represent all conditions of a long haul truck  
360 usage. In the previous 1D model (3.3), each phase is considered, in the rest  
361 of the study, as a driving cycle of approximately the same length (denoted by

Driving cycle	1	2	3	4	5	6	7
Road Type	Extra urban	Highway	Highway	Extra urban	Extra urban	Extra urban	Rolling
Vehicle speed	Medium	High	Medium	Low	Medium	High	High
Weight factor $w_i$ (%)	10	10	50	7.5	10	7.5	5

Table 4: Dynamic evaluation: Driving conditions and weight for the 7 phases

362 a number from 1 to 7) and weighted according to their real life importance  
363 (for a long haul truck highway is predominant).

### 364 4.3. System performance evaluation

365 The criterion used for the performance evaluation under steady state and  
366 dynamic driving conditions, is the total net reinjected power to the conven-  
367 tional driveline. This is done by taking into account the producer (WHRS  
368 expander) and different consumers (cooling fan, WHRS pump and WHRS  
369 coolant pump) and assuming them to be mechanically driven (this is not  
370 always true for the pumps but efficiencies are detuned to take into account  
371 the mechanical to electrical conversion). A complete vehicle model integrat-  
372 ing engine, exhaust after treatment system (EATS), transmission, cooling  
373 package, WHRS and road environment is used to simulate the total vehicle  
374 approach and calculate the power needed to drive the vehicle. The perfor-  
375 mance criterion ( $PC$ ) is then calculated as the ratio of this reinjected power  
376 to the engine power:

$$PC_i = \int_{t_{init}}^{t_{final}} \frac{\dot{W}_{exp} - \dot{W}_{pump} - \dot{W}_{cool,pump} - \dot{W}_{fan}}{\dot{W}_{eng}}, \quad (32)$$

377 where the engine power ( $\dot{W}_{eng}$ ) taking into account the mechanical auxiliaries  
378 consumption mounted on it and the increase in exhaust backpressure (due  
379 to the exhaust evaporator). The vehicle gross weight is assumed constant  
380 and equal to 36 tons which intends to represent the average load on a long  
381 haul truck. The performance criterion ( $PC$ ) over the different steady state  
382 operating points or driving cycles is then calculated by summing the weighted  
383  $PC$  on each points/cycles:

$$PC = \sum_{i=1}^k w_i PC_i, \quad (33)$$

384 where  $k \in [1 \ 13]$  for steady state evaluation (presented in section 4.2.1) and  
385  $k \in [1 \ 7]$  for evaluation on dynamic driving cycle (presented in section 4.2.2).

## 386 5. RESULTS AND DISCUSSION

### 387 5.1. 1D model validation

388 In this section some component models, judged as critical for the overall  
389 system performance evaluation, are first validated thanks to supplier or ex-  
390 perimental data. The different studied configurations being made of the same  
391 components model it has been decided to validate the models components  
392 by components. The validation is done by comparing experimental to the  
393 modeling results. A model is further considered as valid if the average mod-  
394 eling error is below 5% of the predicted quantity. Since the main dynamic of  
395 the system is contained in the evaporators [43] and the final aim is to predict  
396 the power generated by the system only validation figures are presented for  
397 the evaporators and the expansion machine. It should be said that a more  
398 detailed validation on the whole system mounted on the vehicle should be  
399 carried out but this requires the system to be built. Unfortunately this tech-  
400 nology is still under investigation at the truck makers level and no figures  
401 are available yet. This study intends then to compare the architecture and  
402 analyze their impact on the truck fuel consumption.

#### 403 5.1.1. Heat exchangers

404 A high attention is paid to the evaporators in order to accurately predict the  
405 steady state and dynamic performance of those components (corresponding  
406 to the model presented in section 3.3.3). In this paper, a finite volume ap-  
407 proach has been chosen to implement the continuous set of equations (equa-  
408 tions 6, 7, 8, 9). Figure 9 shows the schematic of the discretized model.  
409 Table 5 and 6 show respectively steady state and dynamic prediction errors.  
410 Note that in both cases the relative error is computed according to the max-  
411 imum temperature difference between the heat exchanger bounds (usually  
412  $T_{gL} - T_{f0}$ ). The steady state validation is conducted on a lot of operating  
413 conditions supposed to represent the complete range of operation for those  
414 components. The dynamic behavior is evaluated on different load point varia-  
415 tions but obviously need further validation especially on fast change that can

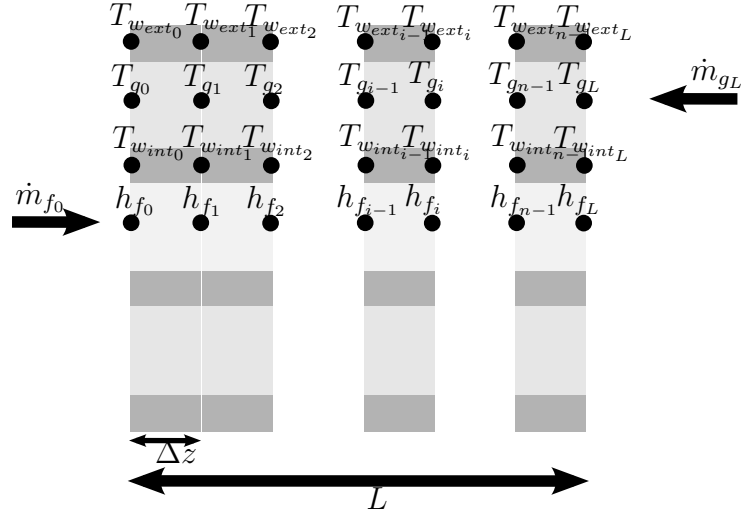


Figure 9: HEX model schematic

416 take place on real driving conditions. However, the mean relative modeling  
 417 error remains lower than 3.5%, which is considered acceptable.

	$T_{f_{LEGRB}}$		$T_{f_{LExhB}}$		$T_{egr0_{EGRB}}$		$T_{exh0_{ExhB}}$	
Error	max	mean	max	mean	max	mean	max	mean
Absolute (K)	2.95	1.30	9.15	4.16	7.54	2.54	15.47	4.71
Relative (%)	0.57	0.29	8.84	3.28	2.34	0.61	8.61	3.40

Table 5: Evaporators steady state validation

	$T_{f_{LEGRB}}$		$T_{f_{LExhB}}$		$T_{egr0_{EGRB}}$		$T_{exh0_{ExhB}}$	
Error	max	mean	max	mean	max	mean	max	mean
Absolute (K)	4.5	1.5	25.9	2.3	7.9	2.8	20	4.2
Relative (%)	1.38	0.46	14.37	1.28	2.43	0.86	11.1	2.33

Table 6: Evaporators dynamic validation

### 418 5.1.2. Expansion machine

419 The turbine expander model presented in 3.3.5 is fitted thanks to supplier  
 420 data. Figure 10 and 11 respectively show the working fluid inlet pressure and  
 421 the generated power predicted by the model versus the normalized working

422 fluid mass flow entering in the turbine. Those two quantities are well fitted  
423 and this model is further considered validated.

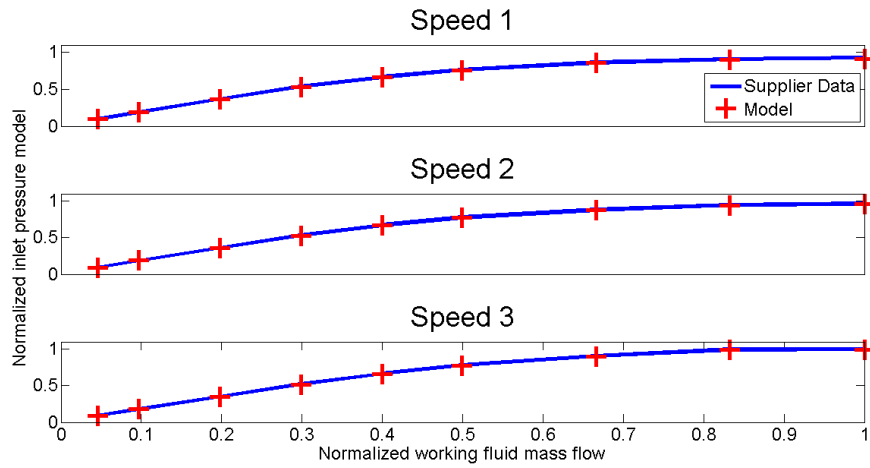


Figure 10: Turbine pressure model validation

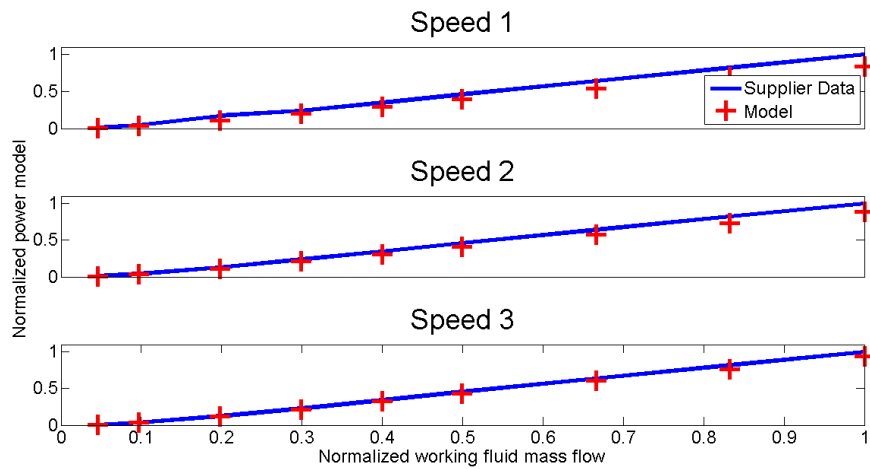


Figure 11: Turbine power model validation

### 424 5.1.3. Model analysis

425 The whole 1D models are built from the same component models. The iner-  
426 tial effect of the pipes are neglected since their effect are negligible compared

427 to the other components dynamics (namely the evaporators) [43]. The full  
428 model is then a combination of validated detailed models (e.g. heat exchang-  
429 ers) and quasi-static models (pumps expansion machine and fan) used for  
430 comparison purpose. This study then intends to compare the different heat  
431 sources and sinks configurations possible on a heavy duty vehicle to select  
432 the best system in terms of performance.

## 433 5.2. Optimization of the WHRS

### 434 5.2.1. Working fluid selection

435 From an exhaustive fluid list [25], all those that do not respect the different  
436 criteria mentioned in 4.1 have been removed. However, as water is a good  
437 reference fluid since it is generally used in power plant [44], it has been kept.  
438 The results presented hereafter are coming from the ideal thermodynamic 0D  
439 model presented in section 3.2 where all 13 operating points are simulated for  
440 two condensing temperatures 60°C and 90°C, which intends to represent the  
441 two cooling configurations presented in the previous section. The parameters  
442 of the cycle,  $P_{f_{out,pump}}$  and  $\dot{m}_f$  are optimized to reach the highest performance  
443 (i.e. maximize the *NOP*). Here, each hot stream is simulated separately in  
444 order to see the impact of the heat source on the Rankine fluid selection. The  
445 simulation matrix contains 13 operating points (listed in section 5.2.2) and  
446 13 selected working fluids. For the sake of simplicity, the results presented  
447 in figure 12 show the number of occurrences where the fluid is in the top  
448 five <sup>1</sup> regarding the *NOP*. When analyzing each operating point and config-  
449 uration separately among the 13x13 simulations, water is the best fluid for  
450 heavily loaded operating points. For low and medium engine load, as gases  
451 temperatures are lower and due to the large enthalpy of vaporization of water  
452 and the high level of superheating required, it is not recommended to use it.  
453 Acetone and ethanol show good performance at mid and high engine load no  
454 matter of the cold sink temperature. Refrigerants such as R1233zd or Novec  
455 649 show good results for heat source temperature under 280 °C for the low-  
456 est condensing temperature. More exotic fluids such as cis-butene or MM  
457 (silicon oil) could be attractive for low and medium engine load respectively  
458 at 60°C condensing temperature for the first one and 90°C for the second one.

459

---

<sup>1</sup>top five means the *NOP* related to the fluid is ranked in one of the five first position

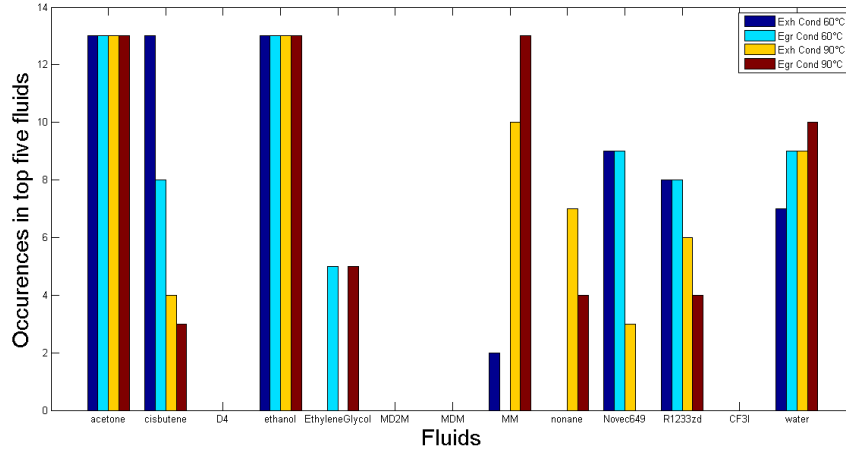


Figure 12: Number of occurrences of each fluid in top five <sup>1</sup> for different boundary conditions

460 These first simulations results limit the number of investigated working fluids  
 461 for the remaining part of this paper to the following ones: Acetone, Ethanol.  
 462 Those two fluids represent the highest number of occurrences for the differ-  
 463 ent configurations considered. As these fluids have similar volumetric flows  
 464 it would be possible to use the same components' characteristics with only  
 465 some minor changes (e.g. throat diameter for the turbine model and pump  
 466 displacement). However due to the low flash point of Acetone (-20°C) only  
 467 ethanol is then considered suitable for a mobile application.

### 468 5.2.2. Steady state performance analysis

469 Now, the performance criterion is analyzed on the 13 operating points and  
 470 the 2 cooling architectures (Cooling config 1 and 2) for the previously cho-  
 471 sen working fluids. The savings are computed thanks to the weight factors  
 472 presented in table 3. Figure 13 presents the NOP to engine power ratio eval-  
 473 uated for the 2 cooling configurations. It can be observed that the decrease  
 474 due to higher condensing temperatures induced by cooling configuration 2 is  
 475 somehow constant (between 11 and 15 %) no matter of the Rankine cycle  
 476 arrangement. This drop in performance is due to the increase in condensing  
 477 pressure which affects the overall pressure ratio through the expansion ma-  
 478 chine and therefore its performance. This could be partially balanced by a

479 specific design of the expansion machine in order to have a variable nozzle ge-  
 480 ometry that keeps the pressure ratio constant when the condensing pressure  
 481 increases. A similar approach is done in [38] to adapt the nozzle geometry to  
 482 the mass flow entering in the turbine. With those components, the parallel  
 483 arrangement of the heat sources gives the best  $PC$ , followed by the serial  
 484 one, the exhaust only and the EGR recovery. However the difference be-  
 485 tween series and parallel layout is not so important and the lower number of  
 486 valves needed by the first one could compensate this drop in performance.  
 487 Moreover, in this configuration, as the working fluid mass flow is controlled  
 488 to get a superheated vapor state at the outlet of the tailpipe boiler the mass  
 489 flow rate is then higher than in any other configurations. It results into lower  
 490 EGR temperature which could be a benefit in terms of engine performance  
 491 and pollutant emission control [4]. Last but not least, with the EGR only  
 492 solution even if the weight and installation impact is low (the heaviest com-  
 493 ponent is the EGR evaporator that replaces the traditional EGR cooler),  
 494 the  $PC$  seems too low for a vehicle installation. This obviously needs further  
 495 analysis taking into account also the cost impact of each solution on the total  
 cost of ownership.

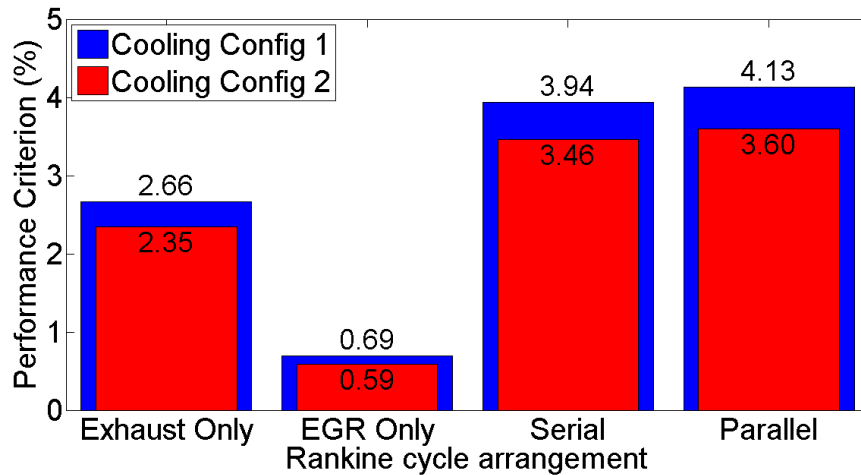


Figure 13: Steady state  $PC$  assessment

496

497 5.2.3. *Dynamic performance analysis*

498 Then, in order to validate the previously used method, dynamic simulations  
 499 are run to further assess the performance criterion of the WHRS. Indeed,  
 500 as previously said, the Rankine based recovery systems could have long time  
 501 constant due to the boiler(s) inertia (wall capacity). This could help in terms  
 502 of control by filtering some high transient of the heat sources but reduce the  
 503 heat transferred to the fluid, since only a fraction of the heat contained in  
 504 the hot gases is then used. In the following, the performance is assessed on  
 505 7 different driving cycles (see table 4) representative of a long haul truck  
 usage. An example of two of those road profiles is presented in fig 14. Each

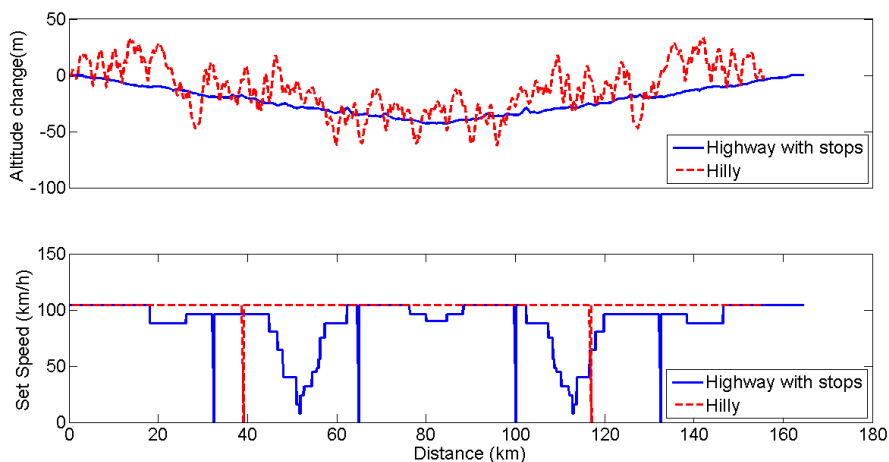


Figure 14: Road profiles examples

506 driving cycle is simulated separately starting from ambient conditions that  
 507 can result in a lower  $PC$  due to the long warm up time of the exhaust after  
 508 treatment system. Weights (see 4) are applied to the different driving cycles  
 509 to calculate the total performance criterion of the WHRS.

510 Figures 15 and 16 show the  $PC$  reached by each Rankine configuration re-  
 511 spectively for cooling configuration 1 and 2. As shown is 5.2.2 the decrease in  
 512 performance using cooling configuration 2 rather than cooling configuration  
 513 1 is more or less constant and around 11%. The main information brought  
 514 by this study remains the lower fuel savings when simulating the system in  
 515 dynamic instead of steady state, which can be as big as 50% for the systems  
 516 using exhaust as heat source. This is due to two main reasons:  
 517

- 518 • the exhaust after treatment system, which has a very important con-  
519 stant time, causes big temperature drop during fast highly loaded en-  
520 gine conditions where a lot of heat is supposed to be available.
- 521 • the non optimal design of the tailpipe boiler used in the simulation  
522 model. Indeed the validation of the model shown in section 5.1 is  
523 based on prototypes components that do not represent the optimum in  
524 terms of size and transient performance.
- 525 • the constraint implemented on the EGR temperature at the evaporator  
526 outlet not to derate the emission control. The maximum EGR temper-  
527 ature is set to 150 °C which on some phases is not going hand in hand  
528 with the superheat level control. The EGR temperature becomes the  
529 control objective and when the superheat is not sufficient the expander  
530 is not fed with working fluid and therefore the power production is null.

531 Table 7 resumes the time (relative to the duty cylce time) where the superheat  
532 is sufficient to feed the expansion vapor. Systems recovering heat from the  
533 exhaust stream mainly suffer from a long start-up phase but then the system  
534 never lose the superheat level needed to expand the working fluid in the  
535 kinetic turbine. This long start-up is due to the boundary conditions used  
536 where all the sub-systems initial temperatures are set to ambient. For the  
537 system recovering heat only from the EGR the start-up is not significant since  
538 on some cycles the system is generating power more than 99% of the time  
539 (the EGR gets its normal operation temperature after few seconds whereas  
540 the thermal inertia of the EATS makes the temperature rise very slow).  
541 Nevertheless on highly loaded cycles (namely 3 and 7) the high engine load  
542 results into high EGR temperature and to not interact too much with the  
543 engine emissions system, the superheat is dropped to the detriment of the  
544 EGR temperature. Superheated vapor is no longer generated by the boiler  
545 and the fluid goes back to a diphasic state and the expansion machine is  
546 bypassed.

547 Anyway, similarly to the previous results in steady state, the best system in  
548 terms of fuel savings remains the EGR and exhaust in parallel with cooling  
549 configuration 1 that brings 2.2% savings on the overall weighted driving cycle.  
550 In addition to that, it can be seen that the relative performance are kept from  
551 arrangement to arrangement (compared to section 5.2.2).

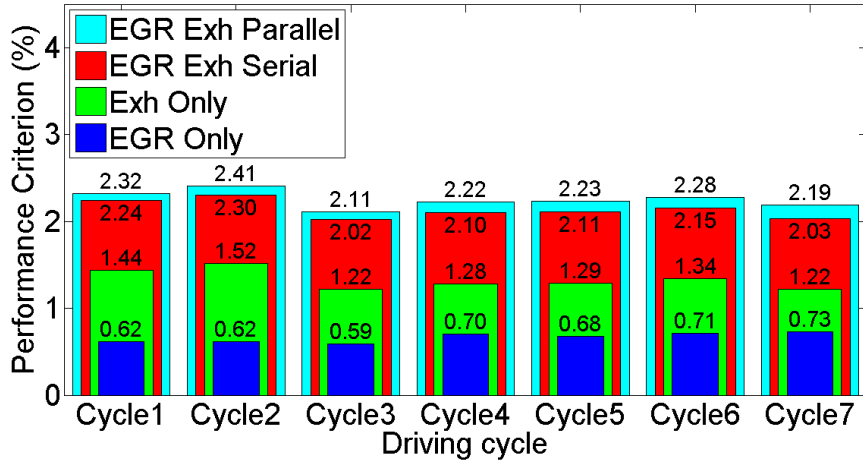


Figure 15: *PC* for cooling configuration 1 over dynamic driving cycles

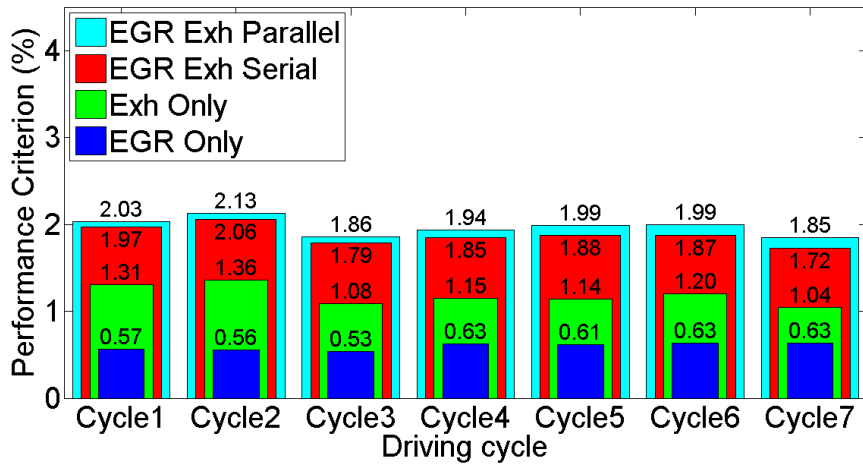


Figure 16: *PC* for cooling configuration 2 over dynamic driving cycles

Configuration	Exhaust	EGR	Serial	Parallel
Driving cycle				
1	93.37 %	99.11%	93.71%	93.93%
2	93.06%	99.30%	93.41%	93.25%
3	95.27%	83.38%	95.64%	95.44%
4	92.50%	93.37%	91.07%	92.06%
5	91.18%	97.26%	90.67%	91.55%
6	92.00%	98.30%	90.42%	91.46%
7	93.53%	88.94%	90.87%	92.92%

Table 7: Vapor creation time ratios summary

552 *5.2.4. Optimal WHRS*

553 The low performance figures presented in the previous sections are mainly  
554 due to non optimized components for the considered application. In order to  
555 evaluate what could be the economy brought by an optimized system, the dif-  
556 ferent components constituting the WHRS are redesigned to perfectly match  
557 the targeted application. In addition to that, a perfect insulation of these  
558 different components is then considered. In this section, only cooling config-  
559 uration 1 is evaluated since it has been shown that it leads to larger savings.  
560 Both approaches previously used (steady state and dynamic analysis) are  
561 presented in figure 17. Optimization has been done on boilers and condenser  
562 size with respect with the additional weight. Pump and expansion machine  
563 performance are increased to reach standards in power plant Rankine cycles  
564 ( $\eta_{pump_{is}} = 70\%$  and  $\eta_{exp_{is,max}} = 78\%$ ). More acceptable results are reached  
565 for a vehicle implementation of such a system, especially when considering a  
566 system recovering from both EGR and exhaust in parallel. Again, a big step  
567 is observed between the two evaluation methodologies which tends to prove  
568 that the cycle division into a certain number of steady state engine operating  
569 points is not adapted for performance evaluation of thermal systems which  
570 generally have a long response time.

571

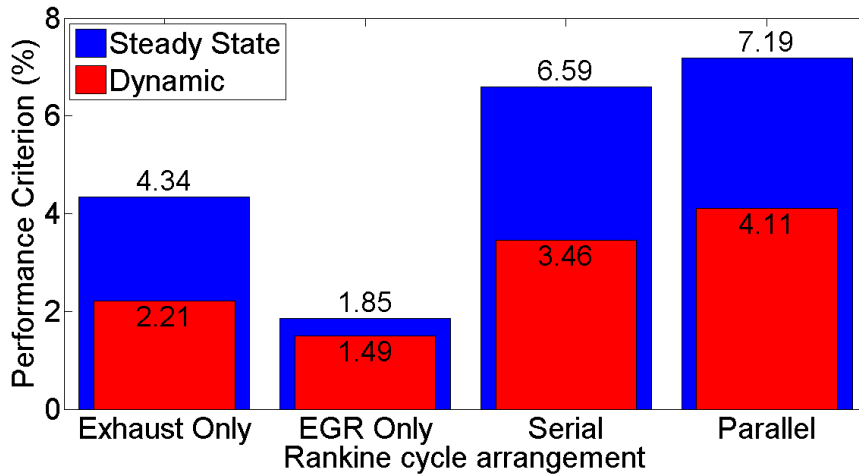


Figure 17: *PC* for optimal sizing of the components

572 **6. CONCLUSION**

573 Performance simulations of different WHRS for heavy duty trucks applica-  
 574 tion was conducted to understand the potential of such a system in terms  
 575 of fuel consumption decrease. Two different methodologies are used and dis-  
 576 cussed. Usually, only the first approach, which consists to split a driving  
 577 cycle into several steady state engine operating points, is used to assess the  
 578 performance without any regards of the transient behavior of the different  
 579 components composing the WHRS [3]. The second one, where a total vehicle  
 580 approach is simulated over a wide variety of dynamic driving cycles repre-  
 581 senting the usage of a long haul HD vehicle. In both methods architecture  
 582 to architecture ranking is the same which tends to prove that the first ap-  
 583 proach could be used for qualitative but not quantitative study. Using the  
 584 second approach results into lower fuel savings and needs to be balanced in  
 585 regards of the model validation done based onto prototypes, which are not  
 586 representing what could be a mass-produced system. However, the absolute  
 587 numbers should not be interpreted as the maximal potential for WHRS in  
 588 HD trucks, since transient control of the system and components are not  
 589 optimal. Different systems layout have been analyzed to maximize the sys-  
 590 tem performance over a broad variety of driving cycles. However the results  
 591 presented in this paper need to be treated carefully and further completed  
 592 with the cost and the packaging effort for each configurations. An optimized

593 scenario is also presented where a specific attention has been paid to the  
594 components size and performance in order to perfectly match the applica-  
595 tion. However fuel savings are rather low compared to what can be found  
596 in the literature [45, 3] and need to be further validated by experimental  
597 results on a system mounted onto a vehicle. In addition to that, control  
598 issues are not approached in this paper but remain a big part of the system  
599 performance maximization. In this study, perfect sensors and actuators are  
600 used, which reduce the control effort. Moreover, actual mass-produced control  
601 units are not as powerful as current laptop central processing unit and  
602 reduce considerably the possibility in terms of advanced control algorithm  
603 development. Recent studies have brought significant advances in this field  
604 [46, 12, 47] but this still needs to be addressed when vehicle implementation  
605 is touched.

## 606 REFERENCES

- 607 [1] P. Patel, E. Doyle, Compounding the truck diesel engine with an or-  
608 ganic rankine-cycle system, in: SAE Technical Paper, no. 760343, SAE  
609 International, 1976.
- 610 [2] S. Oomori, H. Ogino, Waste heat recovery of passenger car using a  
611 combination of rankine bottoming cycle and evaporative cooling system,  
612 in: SAE Technical Paper, no. 930880, SAE International, 1993.
- 613 [3] A. Boretti, Recovery of exhaust and coolant heat with R245fa organic  
614 rankine cycles in a hybrid passenger car with a naturally aspirated gaso-  
615 line engine, *Applied Thermal Engineering* 36 (0) (2012) 73 – 77.
- 616 [4] F. Willems, F. Kupper, R. Cloudt, Integrated powertrain control for  
617 optimal CO<sub>2</sub>-NO<sub>x</sub> tradeoff in an euro-vi diesel engine with waste heat  
618 recovery system, in: *American Control Conference (ACC)*, 2012, 2012,  
619 pp. 1296–1301.
- 620 [5] R. Freymann, W. Strobl, A. Obieglo, The turbosteamer: A system in-  
621 troducing the principle of cogeneration in automotive applications, *MTZ*  
622 *worldwide* 69 (5) (2008) 20–27.
- 623 [6] T. Wang, Y. Zhang, Z. Peng, G. Shu, A review of researches on thermal  
624 exhaust heat recovery with rankine cycle, *Renewable and Sustainable*  
625 *Energy Reviews* 15 (6) (2011) 2862 – 2871.

- 626 [7] C. Sprouse III, C. Depcik, Review of organic rankine cycles for inter-  
627 nal combustion engine exhaust waste heat recovery, *Applied Thermal*  
628 *Engineering* 51 (1–2) (2013) 711 – 722.
- 629 [8] N. Espinosa, Contribution to the study of waste heat recovery systems  
630 on commercial truck diesel engines, Ph.D. thesis, University of Liege,  
631 National Polytechnic Institute of Lorraine (10 2011).
- 632 [9] J. Dickson, M. Ellis, T. Rousseau, J. Smith, Validation and design of  
633 heavy vehicle cooling system with waste heat recovery condenser, *SAE*  
634 *International Journal of Commercial Vehicles* 7 (2014) 458–467.
- 635 [10] E. Wang, H. Zhang, Y. Zhao, B. Fan, Y. Wu, Q. Mu, Performance  
636 analysis of a novel system combining a dual loop organic rankine cycle  
637 (orc) with a gasoline engine, *Energy* 43 (1) (2012) 385 – 395, 2nd Inter-  
638 national Meeting on Cleaner Combustion (CM0901-Detailed Chemical  
639 Models for Cleaner Combustion).
- 640 [11] A. A. Boretti, Transient operation of internal combustion engines with  
641 rankine waste heat recovery systems, *Applied Thermal Engineering* 48  
642 (2012) 18 – 23.
- 643 [12] J. Peralez, P. Tona, O. Lepreux, A. Sciarretta, L. Voise, P. Dufour,  
644 M. Nadri, Improving the control performance of an organic rankine cycle  
645 system for waste heat recovery from a heavy-duty diesel engine using a  
646 model-based approach, in: 52nd Annual IEEE Conference on Decision  
647 and Control (CDC), 2013, pp. 6830–6836.
- 648 [13] S. Quoilin, M. V. D. Broek, S. Declaye, P. Dewallef, V. Lemort, Techno-  
649 economic survey of organic rankine cycle (orc) systems, *Renewable and*  
650 *Sustainable Energy Reviews* 22 (2013) 168 – 186.
- 651 [14] S. Lecompte, H. Huisseune, M. van den Broek, S. D. Schampheleire,  
652 M. D. Paepe, Part load based thermo-economic optimization of the or-  
653 ganic rankine cycle (orc) applied to a combined heat and power (chp)  
654 system, *Applied Energy* 111 (2013) 871 – 881.
- 655 [15] T. A. Horst, W. Tegethoff, P. Eilts, J. Koehler, Prediction of dynamic  
656 rankine cycle waste heat recovery performance and fuel saving potential

- 657 in passenger car applications considering interactions with vehicles' en-  
658 ergy management, *Energy Conversion and Management* 78 (0) (2014)  
659 438 – 451.
- 660 [16] A. Legros, L. Guillaume, M. Diny, H. Zaïdi, V. Lemort, Comparison  
661 and Impact of Waste Heat Recovery Technologies on Passenger Car  
662 Fuel Consumption in a Normalized Driving Cycle, *Energies* 7 (8) (2014)  
663 5273–5290.
- 664 [17] E. Bredel, J. Nickl, S. Bartosch, Waste heat recovery in drive systems of  
665 today and tomorrow, *MTZ worldwide eMagazine* 72 (4) (2011) 52–56.
- 666 [18] R. Freymann, J. Ringler, M. Seifert, T. Horst, The second generation  
667 turbosteamer, *MTZ worldwide* 73 (2) (2012) 18–23.
- 668 [19] S. Flik, M. Edwards, E. Pantow, Emissions reduction in commercial  
669 vehicles via thermomanagement, in: *Proceedings of the 30th wiener*  
670 *motorensymposium*, Viena, Austria, 2009.
- 671 [20] P. J. Mago, L. M. Chamra, C. Somayaji, Performance analysis of dif-  
672 ferent working fluids for use in organic rankine cycles, *Proceedings of*  
673 *the Institution of Mechanical Engineers, Part A: Journal of Power and*  
674 *Energy* 221 (3) (2007) 255–263.
- 675 [21] M. Z. Stijepovic, P. Linke, A. I. Papadopoulos, A. S. Grujic, On the  
676 role of working fluid properties in organic rankine cycle performance,  
677 *Applied Thermal Engineering* 36 (0) (2012) 406 – 413.
- 678 [22] A. I. Papadopoulos, M. Stijepovic, P. Linke, On the systematic design  
679 and selection of optimal working fluids for organic rankine cycles, *Ap-*  
680 *plied Thermal Engineering* 30 (6–7) (2010) 760 – 769.
- 681 [23] E. Cayer, N. Galanis, H. Nesreddine, Parametric study and optimization  
682 of a transcritical power cycle using a low temperature source, *Applied*  
683 *Energy* 87 (4) (2010) 1349 – 1357.
- 684 [24] S. Karellas, A. Schuster, A.-D. Leontaritis, Influence of supercritical  
685 ORC parameters on plate heat exchanger design, *Applied Thermal En-*  
686 *gineering* 33–34 (0) (2012) 70 – 76.

- 687 [25] M. L. H. Eric. W. Lemmon, Refprop nist standard reference database  
688 23 (version 9.0)), thermophysical properties division, national institute  
689 of standards and technology, boulder, co (May 2013).  
690 URL <http://www.nist.gov/srd/nist23.cfm>
- 691 [26] E. Feru, F. Kupper, C. Rojer, X. Seykens, F. Scappin, F. Willems,  
692 J. Smits, B. D. Jager, M. Steinbuch, Experimental validation of a dy-  
693 namic waste heat recovery system model for control purposes, in: SAE  
694 Technical Paper, SAE International, 2013.
- 695 [27] T. A. Horst, H.-S. Rottengruber, M. Seifert, J. Ringler, Dynamic heat  
696 exchanger model for performance prediction and control system design of  
697 automotive waste heat recovery systems, Applied Energy 105 (0) (2013)  
698 293 – 303.
- 699 [28] M. Willatzen, N. Pettit, L. Ploug-Sørensen, A general dynamic sim-  
700 ulation model for evaporators and condensers in refrigeration. part i:  
701 moving-boundary formulation of two-phase flows with heat exchange:  
702 Modèle général dynamique pour évaporateurs et condenseurs frigorifi-  
703 ques. partie i: Formulation des conditions aux limites variables de flux  
704 biphasiques avec échange de chaleur, International Journal of Refrigeration  
705 21 (5) (1998) 398 – 403.
- 706 [29] J. Judge, R. Radermacher, A heat exchanger model for mixtures and  
707 pure refrigerant cycle simulations, International Journal of Refrigeration  
708 20 (4) (1997) 244 – 255.
- 709 [30] S. Bendapudi, J. E. Braun, E. A. Groll, A comparison of moving-  
710 boundary and finite-volume formulations for transients in centrifugal  
711 chillers, International Journal of Refrigeration 31 (8) (2008) 1437 – 1452.
- 712 [31] I. H. Bell, S. Quoilin, E. Georges, J. E. Braun, E. A. Groll, W. T.  
713 Horton, V. Lemort, A generalized moving-boundary algorithm to pre-  
714 dict the heat transfer rate of counterflow heat exchangers for any phase  
715 configuration, Applied Thermal Engineering 79 (2015) 192 – 201.
- 716 [32] I. Vaja, Definition of an object oriented library for the dynamic simula-  
717 tion of advanced energy systems: Methodologies, tools and applications  
718 to combined ice-orc power plants, Ph.D. thesis, University of Parma (05  
719 2009).

- 720 [33] J. R. Thome, Wolverine Tube Inc Engineering Data Book III, Heat  
721 Transfer Databook, Wolverine Tube Inc., 2010.
- 722 [34] J. Bao, L. Zhao, A review of working fluid and expander selections for  
723 organic rankine cycle, *Renewable and Sustainable Energy Reviews* 24  
724 (2013) 325 – 342.
- 725 [35] O. Badr, P. O’Callaghan, S. Probert, Performances of rankine-cycle en-  
726 gines as functions of their expanders’ efficiencies, *Applied Energy* 18 (1)  
727 (1984) 15 – 27.
- 728 [36] A. Costall, A. G. Hernandez, P. Newton, R. Martinez-Botas, Design  
729 methodology for radial turbo expanders in mobile organic rankine cycle  
730 applications, *Applied Energy* (2015) –.
- 731 [37] G. Latz, S. Andersson, K. Munch, Selecting an expansion machine for  
732 vehicle waste-heat recovery systems based on the rankine cycle, in: *SAE*  
733 *Technical Paper*, SAE International, 2013.
- 734 [38] H. Kunte, J. Seume, Partial admission impulse turbine for automotive  
735 orc application, in: *SAE Technical Paper*, SAE International, 2013.
- 736 [39] O. E. Baljé, A study on design criteria and matching of turbomachines:  
737 Part a—similarity relations and design criteria of turbines, *Journal of*  
738 *Engineering Gas Turbines Power* 84 (1) (1962) 83 – 102.
- 739 [40] D. Maraver, J. Royo, V. Lemort, S. Quoilin, Systematic optimization of  
740 subcritical and transcritical organic rankine cycles (orcs) constrained by  
741 technical parameters in multiple applications, *Applied Energy* 117 (0)  
742 (2014) 11 – 29.
- 743 [41] S. Lecompte, H. Huisseune, M. van den Broek, B. Vanslambrouck, M. D.  
744 Paepe, Review of organic rankine cycle (orc) architectures for waste heat  
745 recovery, *Renewable and Sustainable Energy Reviews* 47 (0) (2015) 448  
746 – 461.
- 747 [42] S. Mavridou, G. Mavropoulos, D. Bouris, D. Hountalas, G. Bergeles,  
748 Comparative design study of a diesel exhaust gas heat exchanger for  
749 truck applications with conventional and state of the art heat transfer  
750 enhancements, *Applied Thermal Engineering* 30 (8–9) (2010) 935 – 947.

- 751 [43] R. Stobart, S. Hounsham, R. Weerasinghe, The controllability of vapour  
752 based thermal recovery systems in vehicles, in: SAE Technical Paper,  
753 SAE International, 2007.
- 754 [44] J. Fischer, Comparison of trilateral cycles and organic rankine cycles,  
755 Energy 36 (10) (2011) 6208 – 6219.
- 756 [45] S. Edwards, J. Eitel, E. Pantow, P. Geskes, R. Lutz, J. Tepas, Waste  
757 heat recovery: The next challenge for commercial vehicle thermoman-  
758 agement, SAE International Journal of Commercial Vehicles 5 (2012)  
759 395–406.
- 760 [46] D. Luong, T.-C. Tsao, Linear quadratic integral control of an organic  
761 rankine cycle for waste heat recovery in heavy-duty diesel powertrain,  
762 in: American Control Conference (ACC), 2014, 2014, pp. 3147–3152.
- 763 [47] S. Quoilin, R. Aumann, A. Grill, A. Schuster, V. Lemort, H. Spliethoff,  
764 Dynamic modeling and optimal control strategy of waste heat recovery  
765 organic rankine cycles, Applied Energy 88 (6) (2011) 2183 – 2190.

## 766 APPENDIX

### 767 Nomenclature

#### 768 Acronyms

- 769 *CAC* Charge air cooler  
770 *CFC* Chlorofluorocarbon  
771 *CFD* Computational fluid dynamics  
772 *EATS* Exhaust after treatment system  
773 *EGR* Exhaust gas recirculation  
774 *GADSL* Global automotive declarable substance list  
775 *GWP* Global warming potential  
776 *HCFC* Hydrochlorofluorocarbon  
777 *HD* Heavy duty  
778 *HEX* Heat exchanger  
779 *NFPA* National fire protection agency

780	<i>NOP</i>	Net output power
781	<i>NTU</i>	Number of transfer unit
782	<i>ODP</i>	Ozone depletion potential
783	<i>ORC</i>	Organic Rankine cycle
784	<i>PC</i>	Performance criterion
785	<i>WHRs</i>	Waste heat recovery system
786	<b>Greek letters</b>	
787	$\alpha$	Heat transfer coefficient ( $W/m^2/K$ )
788	$\epsilon$	Heat exchanger efficiency (–)
789	$\eta$	Efficiency (–)
790	$\gamma$	Specific heat ratio (–)
791	$\lambda$	Heat conductivity ( $W/m/K$ )
792	$\omega$	Angular velocity ( $rad/s$ )
793	$\phi$	Compressibility factor (–)
794	$\rho$	Density ( $kg/m^3$ )
795	$\varphi$	Critical pressure ratio (–)
796	<b>Latin letters</b>	
797	$\dot{m}$	Mass flow ( $kg/s$ )
798	$\dot{Q}$	Heat flow rate ( $W$ )
799	$\dot{q}$	Linear heat flow rate ( $W/m$ )
800	$\dot{W}$	Power ( $W$ )
801	$A$	Area ( $m^2$ )
802	$C_c$	Cubic capacity ( $m^3$ )
803	$C_d$	Discharge coefficient (–)
804	$c_p$	Specific heat ( $J/kg/K$ )
805	$G$	Gear ratio (–)
806	$h$	Enthalpy ( $J/kg$ )
807	$K_{eq}$	Equivalent throat diameter ( $m^2$ )
808	$N$	Rotational speed ( $rpm$ )
809	$Nu$	Nusselt number (–)
810	$P$	Pressure ( $Pa$ )
811	$Pe$	Perimeter ( $m$ )

812	<i>PP</i>	Pinch point ( $K$ )
813	<i>r</i>	Ideal gas constant ( $J/kg/K$ )
814	<i>S</i>	Section ( $m^2$ )
815	<i>s</i>	Entropy ( $J/kg/K$ )
816	<i>Sr</i>	Vehicle to ram air speed ratio ( $-$ )
817	<i>T</i>	Temperature ( $K$ )
818	<i>t</i>	Time ( $s$ )
819	<i>V</i>	Volume ( $m^3$ )
820	<i>w</i>	Driving cycle weight ( $-$ )
821	<i>x</i>	Quality ( $-$ )
822	<i>z</i>	Spatial direction ( $m$ )

823 **Subscripts**

824	<i>air</i>	Air
825	<i>amb</i>	Ambient
826	<i>conv</i>	Convection
827	<i>cross</i>	Cross section
828	<i>eff</i>	Effective
829	<i>egr</i>	EGR gas
830	<i>EgrB</i>	EGR boiler
831	<i>eng</i>	Engine
832	<i>exh</i>	Exhaust gas
833	<i>ExhB</i>	Exhaust boiler
834	<i>exp</i>	Expander
835	<i>ext</i>	External wall
836	<i>f</i>	Working fluid
837	<i>fan</i>	Cooling fan
838	<i>g</i>	Gas
839	<i>in</i>	Inlet port
840	<i>int</i>	Internal wall
841	<i>max</i>	Maximum
842	<i>min</i>	Minimum
843	<i>out</i>	Outlet port

844	<i>pump</i>	Pump
845	<i>tank</i>	Tank
846	<i>v</i>	Valve
847	<i>vol</i>	Volumetric
848	<i>wall</i>	Heat exchanger wall